

Including nonlocality in the exchange-correlation kernel from time-dependent current density functional theory: Application to the stopping power of electron liquids

V. U. Nazarov,¹ J. M. Pitarke,^{2,3} Y. Takada,⁴ G. Vignale,⁵ and Y.-C. Chang¹

¹Research Center for Applied Sciences, Academia Sinica, Taipei 115, Taiwan

²CIC nanoGUNE Consolider, Mikeletegi Pasealekua 56, E-2009 Donostia, Basque Country

³Materia Kondentsatuaren Fisika Saila, UPV/EHU and Unidad Fisica de Materiales, CSIC-UPV/EHU, 644 Posta Kutxatila, E-48080 Bilbo, Basque Country

⁴Institute for Solid State Physics, University of Tokyo, Kashiwa, Chiba 277-8581, Japan

⁵Department of Physics and Astronomy, University of Missouri, Columbia, Missouri 65211, USA

(Received 2 March 2007; revised manuscript received 17 September 2007; published 9 November 2007)

We develop a scheme for building the scalar exchange-correlation (XC) kernel of time-dependent density functional theory (TDDFT) from the tensorial kernel of time-dependent *current* density functional theory (TDCDFT) and the Kohn-Sham current density response function. Resorting to the local approximation to the kernel of TDCDFT results in a nonlocal approximation to the kernel of TDDFT, which is free of the contradictions that plague the standard local density approximation (LDA) to TDDFT. As an application of this general scheme, we calculate the dynamical XC contribution to the stopping power of electron liquids for slow ions to find that our results are in considerably better agreement with experiment than those obtained using TDDFT in the conventional LDA.

DOI: 10.1103/PhysRevB.76.205103

PACS number(s): 71.15.Mb, 34.50.Bw

I. INTRODUCTION

Starting with the pioneering work of Runge and Gross,¹ time-dependent density functional theory (TDDFT) has evolved into a powerful tool for studying excitations in atomic, molecular, and condensed-matter systems.²⁻⁶ In the linear-response regime, the key quantity of TDDFT is the dynamical exchange and correlation (XC) kernel $f_{XC}(\mathbf{r}, \mathbf{r}', \omega)$ defined as the Fourier transform with respect to time of the functional derivative

$$f_{XC}(\mathbf{r}, \mathbf{r}', t - t') = \frac{\delta V_{XC}(\mathbf{r}, t)}{\delta n(\mathbf{r}', t')},$$

where V_{XC} and n are the time-dependent XC potential and particle density, respectively. In contrast with the XC potential in static DFT,^{7,8} the dynamical XC potential is strongly nonlocal with respect to space coordinates,⁹ to the point that a local-density approximation (LDA), understood as the zeroth order term in a regular gradient expansion, does not exist. Indeed, the use of LDA to treat genuinely dynamical effects (i.e., effects not captured by the adiabatic approximation) is known to lead to severe contradictions within the theory.¹⁰ Despite impressive successes of TDDFT, there is still the want of a scheme for including nonlocality in XC kernels, accurate enough and practically convenient in applications.⁶

Contrary to ordinary TDDFT, the time-dependent current density functional theory¹¹ (TDCDFT) is known to allow a consistent LDA, which is believed to be of about the same level of accuracy for the time-dependent phenomena as the standard LDA is for ground-state properties. In many concrete applications, however, (including the calculation of the stopping power of electron liquids described below) it is the *scalar* XC kernel of the ordinary TDDFT, rather than the *tensorial* XC kernel of the TDCDFT, that naturally enters the equations describing the many-body effects.

In this paper we exploit the fact that TDDFT and TDCDFT would be completely equivalent if the exact XC functionals were known, to construct a nonlocal approximation for the scalar XC kernel of TDDFT starting from the LDA for the tensorial XC kernel of TDCDFT. As we shall show below, the resulting nonlocal XC kernel of TDDFT satisfies the exact zero-force sum rule, the violation of which within LDA to TDDFT had once provided the motivation for introducing TDCDFT.¹¹

We believe that our nonlocal XC kernel has a broad range of potential applications, particularly in transport theory. As a first demonstration of its usefulness, we present here the results of calculations of the stopping power of an electron liquid for slow ions, wherein we find that the contribution of the many-body dynamical XC effects is not only numerically important, but also leads to better agreement with experiment when the new nonlocal expression for f_{XC} is used in lieu of the conventional LDA.

The organization of this paper is as follows. In Sec. II we derive a formula expressing the exact scalar XC kernel of TDDFT through the exact tensorial XC kernel of TDCDFT and the Kohn-Sham current density response function. In Sec. III we summarize the formal TDDFT of the stopping power of an electron liquid for slow ions and discuss the difficulties the LDA runs into. In Sec. IV we give the details of our calculational procedure and present results and their discussion. Section V contains our conclusions. The appendix is devoted to the interrelations between scalar and tensorial zero-force sum rules within the exact and approximate theories.

II. SCALAR XC KERNEL OF TDDFT FROM THE TENSORIAL XC KERNEL OF TDCDFT

We start from the expression of the XC kernel of TDDFT (Ref. 12) (the dependence on \mathbf{r} , \mathbf{r}' , and ω is implied)

$$f_{\text{XC}} = \chi_{\text{KS}}^{-1} - \chi^{-1} - \frac{1}{|\mathbf{r} - \mathbf{r}'|}, \quad (1)$$

where χ is the longitudinal density response function and χ_{KS} is its single-particle Kohn-Sham (KS) counterpart. Similarly,¹¹

$$\hat{f}_{\text{XC},ij} = \hat{\chi}_{\text{KS},ij}^{-1} - \hat{\chi}_{ij}^{-1} - \frac{c}{\omega^2} \nabla_i \frac{1}{|\mathbf{r} - \mathbf{r}'|} \nabla_j', \quad (2)$$

where $\hat{f}_{\text{XC},ij}$ is the tensorial XC kernel of the TDCDFT, $\hat{\chi}_{ij}$ and $\hat{\chi}_{\text{KS},ij}$ are the many-body current density response function and its single-particle KS counterpart, respectively. Inverting the relation between the tensorial current density and the scalar density response functions

$$\chi = -\frac{c}{\omega^2} \nabla_i \cdot \hat{\chi}_{ij} \cdot \nabla_j', \quad (3)$$

we can write

$$\chi^{-1} = -\frac{\omega^2}{c} \nabla^{-2} \nabla \cdot (\hat{L} \hat{\chi} \hat{L})^{-1} \cdot \nabla \nabla^{-2},$$

where \hat{L} is the longitudinal projector operator $\hat{L}_{ij} = \nabla_i \nabla_j \nabla^{-2}$. Using a simple operator identity

$$(\hat{L} \hat{\chi} \hat{L})^{-1} = \hat{L} \hat{\chi}^{-1} \hat{L} - \hat{L} \hat{\chi}^{-1} (\hat{T} \hat{\chi}^{-1} \hat{T})^{-1} \hat{\chi}^{-1} \hat{L},$$

where $\hat{T} = \hat{1} - \hat{L}$ is the transverse projector, we can write for the inverse scalar response function

$$\chi^{-1} = -\frac{\omega^2}{c} \nabla^{-2} \nabla \cdot [\hat{\chi}^{-1} - \hat{\chi}^{-1} (\hat{T} \hat{\chi}^{-1} \hat{T})^{-1} \hat{\chi}^{-1}] \cdot \nabla \nabla^{-2} \quad (4)$$

and similarly for χ_{KS} . Using Eqs. (1), (2), (4), and the KS counterpart of the latter, we readily arrive at

$$f_{\text{XC}} = -\frac{\omega^2}{c} \nabla^{-2} \nabla \cdot \{ \hat{f}_{\text{XC}} + (\hat{\chi}_{\text{KS}}^{-1} - \hat{f}_{\text{XC}}) [\hat{T} (\hat{\chi}_{\text{KS}}^{-1} - \hat{f}_{\text{XC}}) \hat{T}]^{-1} \\ \times (\hat{\chi}_{\text{KS}}^{-1} - \hat{f}_{\text{XC}}) - \hat{\chi}_{\text{KS}}^{-1} (\hat{T} \hat{\chi}_{\text{KS}}^{-1} \hat{T})^{-1} \hat{\chi}_{\text{KS}}^{-1} \} \cdot \nabla \nabla^{-2}. \quad (5)$$

Equation (5) is our desired and central result: It expresses the scalar XC kernel of TDDFT in terms of its tensorial counterpart of TDCDFT.

In the case of a *bounded* system, the exact scalar XC kernel satisfies the zero-force sum rule¹⁰

$$\int f_{\text{XC}}(\mathbf{r}, \mathbf{r}', \omega) \nabla' n_0(\mathbf{r}') d\mathbf{r}' = \nabla V_{\text{XC}}(\mathbf{r}), \quad (6)$$

where $n_0(\mathbf{r})$ and $V_{\text{XC}}(\mathbf{r})$ are, respectively, the ground-state density and the XC potential. On the other hand, the tensorial \hat{f}_{XC} and $\hat{\chi}_{\text{KS}}$ satisfy the corresponding sum rules of TDCDFT.¹³ In the Appendix we prove an important result that with any *approximation* to the tensorial \hat{f}_{XC} satisfying the zero-force sum rule, the corresponding scalar XC kernel of Eq. (5) satisfies the sum rule (6).

III. TDDFT OF THE STOPPING POWER OF ELECTRON LIQUID

We now illustrate the usefulness of Eq. (5) by applying it to the problem of the stopping power of an electron liquid for slow ions.

A. Formal TDDFT of the stopping power of electron liquid for a slow ion

The stopping power dE/dx is the loss of energy per unit path of an ion moving through the electron liquid. The constant of proportionality between dE/dx and the ion velocity (for low velocity) defines the *friction coefficient* Q , which can be written as¹⁴

$$Q = Q_1 + Q_2,$$

where Q_1 and Q_2 are the single-particle and the many-body dynamical XC contributions, respectively. The single-particle (binary-collisions) contribution Q_1 can be expressed as¹⁵⁻¹⁸

$$Q_1 = \bar{n}_0 k_F \sigma_{\text{tr}}(k_F), \quad (7)$$

where k_F is the Fermi wave number, $\sigma_{\text{tr}}(k_F)$ is the transport cross section of the elastic scattering in the KS potential of an electron at the Fermi level, and \bar{n}_0 is the electron liquid density in the absence of the ion. As shown in Ref. 14, keeping the Q_1 part of the friction coefficient only is equivalent to using the *adiabatic* version of TDDFT.

The many-body dynamical XC contribution Q_2 is given by¹⁴

$$Q_2 = - \int [\nabla_{\mathbf{r}} n_0(\mathbf{r}) \cdot \hat{\mathbf{v}}] [\nabla_{\mathbf{r}'} n_0(\mathbf{r}') \cdot \hat{\mathbf{v}}] \\ \times \frac{\partial \text{Im} f_{\text{XC}}(\mathbf{r}, \mathbf{r}', \omega)}{\partial \omega} \Big|_{\omega=0} d\mathbf{r} d\mathbf{r}', \quad (8)$$

where $f_{\text{XC}}(\mathbf{r}, \mathbf{r}', \omega)$ is the scalar XC kernel of the inhomogeneous many-body system of an ion at rest in electron liquid and $\hat{\mathbf{v}}$ is the unit vector in the direction of the ion velocity.

In the following, we focus on the calculation of Q_2 .

B. Contradiction inherent in the LDA

The simplest approximation, namely the LDA to the ordinary TDDFT,¹² amounts to setting

$$f_{\text{XC}}(\mathbf{r}, \mathbf{r}', \omega) = f_{\text{XC},L}^h[n_0(r), \omega] \delta(\mathbf{r} - \mathbf{r}'), \quad (9)$$

where $f_{\text{XC},L}^h(n, \omega)$ is the $q \rightarrow 0$ limit of the longitudinal XC kernel of a homogeneous electron liquid of density n . By spherical symmetry, substitution of Eq. (9) into Eq. (8) yields

$$Q_2 = -\frac{4\pi}{3} \int_0^\infty dr [r n_0'(r)]^2 \frac{\partial \text{Im} f_{\text{XC},L}^h[n_0(r), \omega]}{\partial \omega} \Big|_{\omega=0}. \quad (10)$$

In the limit of zero density of the electron liquid $\bar{n}_0 \rightarrow 0$, the independent-electron part Q_1 of Eq. (7) vanishes, but Q_2 of Eq. (10) gives a finite value, because the gradient of the

TABLE I. Inaccuracy of LDA to TDDFT: Friction coefficient of free space ($r_s = \infty$) and that of an electron liquid of $r_s = 2.2$ for several atoms. Line 3 is the ratio of lines 1 and 2 (%).

Atom	He	Be	C	O	Ne	Mg	Si
$Q(r_s = \infty)$	0.04	0.11	0.17	0.24	0.30	0.36	0.43
$Q(r_s = 2.2)$	0.34	0.43	0.70	0.46	0.16	0.15	0.54
%	12	25	24	52	188	240	80

ground-state density $n_0(r)$ of an isolated atom is not zero and $\partial \text{Im} f_{\text{XC},L}^h(n, \omega) / \partial \omega|_{\omega=0}$ is negative.¹⁹ Thus LDA to the scalar f_{XC} yields a finite friction coefficient even in the absence of the electron gas, indicating an obvious flaw of the approximation. Table I shows this error quantitatively for a number of atoms in comparison with friction coefficient at $r_s = 2.2$.

To check that Eq. (5) resolves this problem of the finite friction coefficient of free space, it is sufficient to notice that an isolated atom is a bounded system and hence the sum rule (6) holds, which, substituted into Eq. (8), yields zero identically. Moreover, LDA to TDCDFT satisfies the zero-force sum rule by construction,¹¹ ensuring, as is shown in the Appendix, that Eq. (6) holds for a bounded system even if the local version of TDCDFT is used in Eq. (5).²⁸

IV. CALCULATIONAL PROCEDURE, RESULTS, AND DISCUSSION

Our numerical procedure is to evaluate and invert operators entering Eq. (5) on an orthonormal set of radial basis functions. For $\hat{\chi}_{\text{KS},ij}$, we have employed the standard method of using the static KS orbitals to build the independent-electron response function

$$\begin{aligned} \hat{\chi}_{\text{KS},ij}(\mathbf{r}, \mathbf{r}', \omega) &= \frac{1}{c} n_0(\mathbf{r}) \delta(\mathbf{r} - \mathbf{r}') \delta_{ij} - \frac{1}{4c} \\ &\times \sum_{\alpha\beta} \frac{f_\alpha - f_\beta}{\omega - \epsilon_\beta + \epsilon_\alpha + i\eta} [\psi_\alpha^*(\mathbf{r}) \nabla_i \psi_\beta(\mathbf{r}) \\ &- \psi_\beta(\mathbf{r}) \nabla_i \psi_\alpha^*(\mathbf{r})] \times [\psi_\beta^*(\mathbf{r}') \nabla'_j \psi_\alpha(\mathbf{r}') \\ &- \psi_\alpha(\mathbf{r}') \nabla'_j \psi_\beta^*(\mathbf{r}')], \end{aligned} \quad (11)$$

where $\psi_\alpha(\mathbf{r})$ and ϵ_α are the single-particle wave function and eigenenergy, respectively, in the state α , and f_α is the occupation number of this state. For $\hat{f}_{\text{XC},ij}$, we use LDA to TDCDFT as²⁰

$$\begin{aligned} \int f_{\text{XC},ik}(\mathbf{r}, \mathbf{r}', \omega) j_k(\mathbf{r}') d\mathbf{r}' &= \frac{ic}{\omega} \times \left[-\nabla_i V_{\text{XC}}^{\text{ALDA}}(\mathbf{r}, \omega) \right. \\ &\left. + \frac{1}{n_0(\mathbf{r})} \nabla_k \sigma_{\text{XC},ik}(\mathbf{r}, \omega) \right], \end{aligned} \quad (12)$$

where

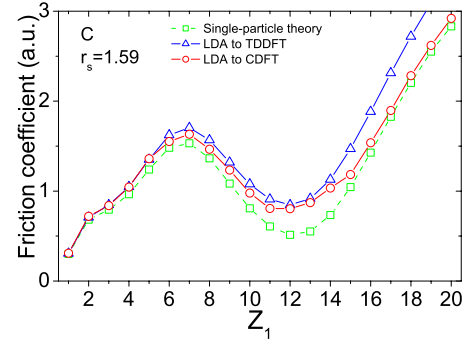


FIG. 1. (Color online) Friction coefficient of electron liquid of carbon density ($r_s = 1.59$) vs the atomic number of an ion. Green squares are results with neglect of the dynamical XC [Eq. (7)]. Triangles are results with the dynamical XC included within LDA to the conventional TDDFT [Eq. (10)]. Circles are results with the dynamical XC included with use of Eqs. (5) and (12)–(15).

$$V_{\text{XC}}^{\text{ALDA}}(\mathbf{r}, \omega) = \frac{1}{i\omega} \epsilon_{\text{XC}}''[n_0(\mathbf{r})] \nabla_k j_k(\mathbf{r}), \quad (13)$$

$\epsilon_{\text{XC}}(n)$ is the XC energy density,

$$\begin{aligned} \sigma_{\text{XC},ik}(\mathbf{r}, \omega) &= \tilde{\eta}_{\text{XC}}[n_0(\mathbf{r}), \omega] \left[\nabla_k u_i(\mathbf{r}) + \nabla_i u_k(\mathbf{r}) \right. \\ &\left. - \frac{2}{3} \nabla_s u_s(\mathbf{r}) \delta_{ik} \right] + \tilde{\zeta}_{\text{XC}}[n_0(\mathbf{r}), \omega] \nabla_s u_s(\mathbf{r}) \delta_{ik}, \end{aligned} \quad (14)$$

is the stress tensor, and $\mathbf{u}(\mathbf{r}) = \mathbf{j}(\mathbf{r}) / n_0(\mathbf{r})$ is the velocity field. The viscosity coefficients are given by²⁹

$$\begin{aligned} \tilde{\zeta}_{\text{XC}}(n, \omega) &= -\frac{n^2}{i\omega} \left[f_{\text{XC},L}^h(n, \omega) - \frac{4}{3} f_{\text{XC},T}^h(n, \omega) - \epsilon_{\text{XC}}''(n) \right], \\ \tilde{\eta}_{\text{XC}}(n, \omega) &= -\frac{n^2}{i\omega} f_{\text{XC},T}^h(n, \omega), \end{aligned} \quad (15)$$

and $f_{\text{XC},T}^h(n, \omega)$ is the transverse XC kernel of the homogeneous electron liquid of density n .

In Fig. 1, we plot the results at $r_s = 1.59$ corresponding to the valence electron-density of carbon.³⁰ It is instructive that within $1 \leq Z_1 \leq 14$ both TDCDFT and TDDFT give virtually the same result, which, we believe, is generally true for light atoms in high-density electron liquid. Then, at higher Z_1 , rather abruptly, the dynamical XC contribution almost vanishes in our present calculation, which can be understood qualitatively recalling that for heavy atoms in the electron liquid the charge-density distribution is close to that of isolated atoms, and hence Q_2 should be small.

In order to compare our result with experiment, we plot the friction coefficient at $r_s = 2.2$ versus the atomic number of a moving ion in Fig. 2. Results of the calculations with neglect of the dynamical XC [Eq. (7)], LDA to TDDFT [the sum of Eq. (7) and Eq. (10)], and LDA to TDCDFT [the sum of Eq. (7) and Eq. (8) with f_{XC} given by Eqs. (5) and (12)–(15)] are shown, together with the experimental data of Ref.

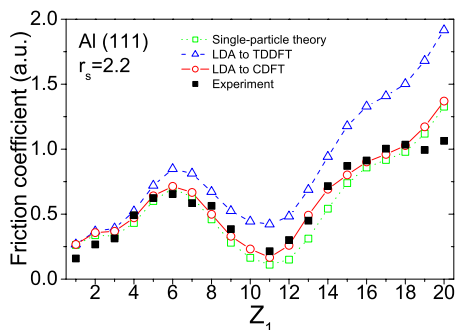


FIG. 2. (Color online) Friction coefficient of electron liquid of $r_s=2.2$ vs the atomic number of an ion. The squares are the results with neglect of the dynamical XC as obtained from Eq. (7). Triangles are the results with the dynamical XC included within LDA to the conventional TDDFT as obtained from Eq. (10). Circles are results with the dynamical XC included with use of Eq. (5) for XC kernel and Eqs. (12)–(15) of LDA to TDCDFT. Solid squares are the measured stopping power of Al of Ref. 21 for ions ($v=0.5$ a.u.) moving at a distance of 1.2 a.u. from the last atomic plane of the Al (111) surface.

21 for ions moving with the velocity of 0.5 a.u. at the distance of 1.2 a.u. from the last atomic plane of the (111) surface of aluminum. The inhomogeneity of the electron density an ion travels through is weak under these conditions, and we have used r_s estimated experimentally.²¹ Moreover, the experimental stopping power is predominantly electronic since the trajectory of an ion is well separated from the lattice atoms. All together, these two conditions justify the comparison with the theory within the electron liquid model. The nonmonotonic dependence of the friction coefficient on the atomic number of the ion (so-called Z_1 oscillations) is known to result within the single-particle theory from the competition between the increase in the electron liquid-ion interaction with the growing charge of the nucleus of the ion and its decrease due to the screening by shells of bounded electrons of the pseudoatom as well as its resonant states.¹⁸

While LDA to TDDFT (triangles in Fig. 2) largely overestimates the friction coefficient at $Z_1 \geq 5$, the results using Eq. (5) (circles in Fig. 2) are in good agreement with the experiment in a wide range of $3 \leq Z_1 \leq 18$. A deviation occurs at small and large Z_1 , where the experimental friction coefficient is *lower* than the independent-electrons calculations (open squares in Fig. 2). This feature has recently been reported as due to the finite velocity of ions.²² Hence it is an effect of the deviation from linear dependence of stopping power on velocity. The same effect gives a *positive* contribution at $8 \leq Z_1 \leq 12$, suggesting that combined with the many-body effects of the present theory the agreement with experiment can be further improved.³¹ In the range $13 \leq Z_1 \leq 17$, the dynamical many-body effects seem to be solely responsible for the enhancement of the friction coefficient compared with the independent-electron theory.

In Fig. 3, we plot the friction coefficient at $r_s=2$ versus the atomic number of ions in the range $5 \leq Z_1 \leq 39$. This is compared with the available measured stopping power for ions with the velocity of 0.68 a.u. channeled along the (110) direction in gold. Due to the channeling, collisions with the

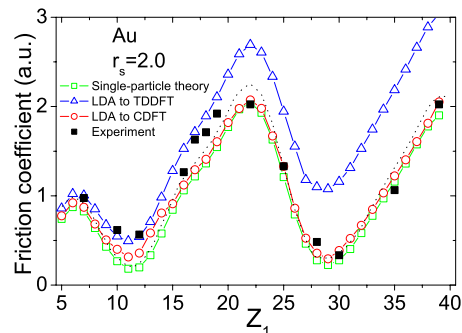


FIG. 3. (Color online) Friction coefficient of electron liquid of $r_s=2$ versus the atomic number of an ion. Squares are the results with neglect of the dynamical XC [Eq. (7)]. Triangles are the results with the dynamical XC included within LDA to the conventional TDDFT [Eq. (10)]. Circles are results with the dynamical XC included with use of Eqs. (5) and (12)–(15). Solid squares are the measurements from Ref. 23 of stopping power of Au for ions ($v=0.68$ a.u.) channeled along the (110) direction. The dotted line is the calculation of Ref. 24 with the dynamical XC included within the linear-response theory of the homogeneous electron gas.

lattice atoms again do not give significant contribution to the stopping power. It must be noted, however, that under channeling conditions the assumption of the nearly constant electron density is an uncontrolled approximation. One important qualitative conclusion we can draw from comparison of the theory and experiment in this case is that for $Z_1 \geq 22$ the role of dynamical XC effects becomes negligible in both experiment and the present theory, while LDA to the TDDFT yields these effects largely overestimated. Similar to the dip in Fig. 2, the underestimated theoretical values at $7 \leq Z_1 \leq 12$ can be attributed to the effect of finite velocity.²² However, within the range $16 \leq Z_1 \leq 19$ the dynamical XC contribution is too small to account for the onset at the experimental data, nor can the persistent enhancement of the friction coefficient in this range be attributed to the effect of finite velocity within the independent-particle theory. Further studies are required to elucidate the nature of this onset, the inhomogeneity of electron density being the most plausible cause. The dotted line in Fig. 3 represents the friction coefficient of silver obtained with the dynamical electron-electron interactions included in Ref. 25 within the framework of the linear-response theory of the homogeneous electron gas. In the case of the nondegenerate plasma, an approach similar to that of Ref. 25 has been reported in Refs. 26 and 27.

V. CONCLUSIONS

We have rigorously expressed the dynamical XC kernel $f_{XC}(\mathbf{r}, \mathbf{r}', \omega)$ of TDDFT in the terms of its TDCDFT tensorial counterpart and the Kohn-Sham current density response function of independent electrons. Then, using the local density approximation to TDCDFT, we have built a nonlocal approximation to $f_{XC}(\mathbf{r}, \mathbf{r}', \omega)$ which satisfies the exact zero-force sum rule for bounded systems. We believe that our new approximation will be broadly applicable to a variety of problems in electronic transport theory.

As a first application, we have calculated the dynamical XC contribution to the stopping power of an electron liquid for slow ions. In doing so we have resolved a basic difficulty of the conventional LDA—the finite friction coefficient of free space—and we have improved the overall agreement between theory and experiment.

ACKNOWLEDGMENTS

G.V. and Y.T. acknowledge, respectively, financial support by the Department of Energy Grant No. DE-FG02-05ER46203 and a Grant-in-Aid for Scientific Research in Priority Areas (No.17064004) of MEXT, Japan.

APPENDIX: RELATION BETWEEN SCALAR AND TENSORIAL ZERO-FORCE SUM RULES

The following sum rules hold¹³ for the exact tensorial XC kernel

$$\int \hat{f}_{XC,ij}(\mathbf{r}, \mathbf{r}', \omega) n_0(\mathbf{r}') d\mathbf{r}' = -\frac{c}{\omega^2} \nabla_i \nabla_j V_{XC}(\mathbf{r}) \quad (\text{A1})$$

and for the KS and the interacting current density response functions, respectively,

$$\begin{aligned} & \frac{c}{\omega^2} \int \hat{\chi}_{KS,ik}(\mathbf{r}, \mathbf{r}', \omega) \nabla'_k \nabla'_j V_{KS}(\mathbf{r}') d\mathbf{r}' \\ & = c \int \hat{\chi}_{KS,ij}(\mathbf{r}, \mathbf{r}', \omega) d\mathbf{r}' - n_0(\mathbf{r}) \delta_{ij}, \end{aligned} \quad (\text{A2})$$

$$\begin{aligned} & \frac{c}{\omega^2} \int \hat{\chi}_{ik}(\mathbf{r}, \mathbf{r}', \omega) \nabla'_k \nabla'_j V_0(\mathbf{r}') d\mathbf{r}' \\ & = c \int \hat{\chi}_{ij}(\mathbf{r}, \mathbf{r}', \omega) d\mathbf{r}' - n_0(\mathbf{r}) \delta_{ij}, \end{aligned} \quad (\text{A3})$$

where $V_0(\mathbf{r})$ is the bare potential.

In this appendix, we prove that for any *approximation* to \hat{f}_{XC} satisfying the sum rule (A1), the corresponding scalar f_{XC} obtained through Eq.(5) satisfies the sum rule of Eq. (6). First, the validity of Eq. (A2) is independent on an approximation for \hat{f}_{XC} , and it can be verified directly with use of the explicit representation of $\hat{\chi}_{KS}$ of Eq. (11). Second, Eq. (A3) holds if Eqs. (A1) and (A2) hold as can be seen by easily inverting the arguments of Ref. 13 leading from Eqs. (A2) and (A3) to Eq. (A1). Equation (A3) can be rewritten as

$$\begin{aligned} & \frac{c}{\omega^2} \int \hat{\chi}_{ik}(\mathbf{r}, \mathbf{r}', \omega) \nabla'_k \nabla'_j V_0(\mathbf{r}') d\mathbf{r}' \\ & = c \int \hat{\chi}_{ik}(\mathbf{r}, \mathbf{r}', \omega) \nabla'_k r'_j d\mathbf{r}' - n_0(\mathbf{r}) \delta_{ij}. \end{aligned} \quad (\text{A4})$$

The next step involves integration by parts requiring the response function to vanish at infinity and, therefore, it applies to bounded systems only. In this case we can write multiplying Eq. (A4) scalarly from the left by ∇ and using Eq. (3)

$$\int \chi(\mathbf{r}, \mathbf{r}', \omega) [\omega^2 r'_j - \nabla'_j V_0(\mathbf{r}')] d\mathbf{r}' = \nabla_j n_0(\mathbf{r}),$$

and after the inversion

$$\int \chi^{-1}(\mathbf{r}, \mathbf{r}', \omega) \nabla_j n_0(\mathbf{r}') d\mathbf{r}' = \omega^2 r_j - \nabla_j V_0(\mathbf{r}). \quad (\text{A5})$$

A similar relation holds for χ_{KS}

$$\int \chi_{KS}^{-1}(\mathbf{r}, \mathbf{r}', \omega) \nabla_j n_0(\mathbf{r}') d\mathbf{r}' = \omega^2 r_j - \nabla_j V_{KS}(\mathbf{r}). \quad (\text{A6})$$

Subtracting Eq. (A5) from Eq. (A6) and using the definition of Eq. (1), we immediately arrive at Eq. (6).

-
- ¹E. Runge and E. K. U. Gross, Phys. Rev. Lett. **52**, 997 (1984).
²M. Petersilka, U. J. Gossmann, and E. K. U. Gross, Phys. Rev. Lett. **76**, 1212 (1996).
³A. Wasserman, N. T. Maitra, and K. Burke, Phys. Rev. Lett. **91**, 263001 (2003).
⁴L. Reining, V. Olevano, A. Rubio, and G. Onida, Phys. Rev. Lett. **88**, 066404 (2002).
⁵A. Marini, R. Del Sole, and A. Rubio, Phys. Rev. Lett. **91**, 256402 (2003).
⁶K. Burke, J. Werschnik, and E. K. U. Gross, J. Chem. Phys. **123**, 062206 (2005).
⁷P. Hohenberg and W. Kohn, Phys. Rev. **136**, B864 (1964).
⁸W. Kohn and L. J. Sham, Phys. Rev. **140**, A1133 (1965).
⁹J. P. Perdew and M. Levy, Phys. Rev. Lett. **51**, 1884 (1983).
¹⁰G. Vignale, Phys. Lett. A **209**, 206 (1995).
¹¹G. Vignale and W. Kohn, Phys. Rev. Lett. **77**, 2037 (1996).
¹²E. K. U. Gross and W. Kohn, Phys. Rev. Lett. **55**, 2850 (1985).
¹³G. Vignale and W. Kohn, in *Electronic Density Functional*

- Theory: Recent Progress and New Directions*, edited by J. Dobson, M. P. Das, and G. Vignale (Plenum Press, New York, 1998).
¹⁴V. U. Nazarov, J. M. Pitarke, C. S. Kim, and Y. Takada, Phys. Rev. B **71**, 121106(R) (2005).
¹⁵J. Finneman, Ph.D. thesis, Aarhus University, the Institute of Physics, 1968.
¹⁶T. L. Ferrell and R. H. Ritchie, Phys. Rev. B **16**, 115 (1977).
¹⁷P. M. Echenique, R. M. Nieminen, and R. H. Ritchie, Solid State Commun. **37**, 779 (1981).
¹⁸P. M. Echenique, R. M. Nieminen, J. C. Ashley, and R. H. Ritchie, Phys. Rev. A **33**, 897 (1986).
¹⁹Z. Qian and G. Vignale, Phys. Rev. B **65**, 235121 (2002).
²⁰G. Vignale, C. A. Ullrich, and S. Conti, Phys. Rev. Lett. **79**, 4878 (1997).
²¹H. Winter, J. I. Juaristi, I. Nagy, A. Arnau, and P. M. Echenique, Phys. Rev. B **67**, 245401 (2003).
²²R. Vincent and I. Nagy, Nucl. Instrum. Methods Phys. Res. B **256**, 182 (2007).

- ²³J. Böttiger and F. Bason, *Radiat. Eff.* **2**, 105 (1969).
- ²⁴I. Nagy, A. Arnau, and P. M. Echenique, *Phys. Rev. A* **40**, 987 (1989).
- ²⁵I. Nagy, A. Arnau, P. M. Echenique, and E. Zaremba, *Phys. Rev. B* **40**, R11983 (1989).
- ²⁶K. Morawetz and G. Röpke, *Phys. Rev. E* **54**, 4134 (1996).
- ²⁷A. Selchow and K. Morawetz, *Phys. Rev. E* **59**, 1015 (1999).
- ²⁸Notice that the sum rule (6) *does not hold* for an *extended* system: This is why Q_2 is different from zero for an electron liquid of finite density.
- ²⁹We have used the zero-temperature viscosities, which are valid for $\omega \gg T^2/E_F$. This is justified since in the experimentally accessible regime $\omega \sim 0.1$ a.u. and $T^2/E_F \sim 10^{-6}$ a.u. at room temperature.
- ³⁰The available experimental stopping power of carbon [D. Ward *et al.*, *Can. J. Phys.* **57**, 645 (1979); G. Högberg, *Phys. Status Solidi B* **46**, 829 (1971)] is predominantly determined by collisions with lattice atoms, making it meaningless to compare with electron gas model calculations.
- ³¹Reference 22 attributes the overestimation by Ref. 14 of the role of the many-body effects to the use of the *total* ground-state density rather than that of the delocalized states only. The total density is, however, the basic variable of TDDFT and without any assumptions it enters the rigorous result of Eq. (8). The real source of the overestimation of the dynamical XC in Ref. 14 was, as Ref. 14 had anticipated and the present work shows, use of LDA within TDDFT.